AA19 - Extended Operation Experience of Superhex High Corrosion Resistance Low Carbon Steel at Alumina Refineries

Darwin Del Aguila[1], Joseph Del Aguila[2]
1. Corrosion Scientist
2. Director
Aushex Pty Ltd, Brisbane, Australia
Corresponding author: d.delaguila@aushex.com

Abstract

Superhex is a low-carbon steel tube metallurgically engineered to provide high acid corrosion resistance by the formation of a strong passive film. This material has been exposed to the alumina refinery process condition for the first time in January 2021. Until now, this material is being trailed in Australia, Brazil, and Canada. In Australia, corrosion performance was monitored during the acid wash and Bayer liquor using a corrosion probe positioned between two live steam heater**s** (LSH) of an evaporation train, and the corrosion rate (mmpy) was measured from electrochemistry data of linear polarization resistance (LPR) and Impedance. The results consistently showed more corrosion resistance (less corrosion attack) of Superhex against the STD alumina refinery tube and other similar materials in the market. After more than two years (2) into operation, specific Hex units containing both the STD refinery and Superhex tubes, were recently opened for visual comparative inspection. Pictures were taken and will be made available for presentation. The initial electrochemistry assessment has also been confirmed by the low maintenance work records so far observed on these units compared with the ones containing the STD refinery HEX tubes. The life span of Superhex is expected to be higher than the STD alumina refinery tube. Because of its inherent property of forming a passive film in contact with sulphuric and hydrochloric acid in any form, this material is been explored to be used in other forms (sheets, vessels) and industries (fertilizer, power stations, etc.) that use these acids as part of their operations. Its corrosion mechanism has been identified as Diffusion Control of Cathodic Reaction unlikely the STD refinery and other ASTM 179 tubes that are Activation Mechanism.

Keywords: Superhex, Sulphuric acid, Corrosion resistance, ASTM 179, Heat exchanger tube.

1. Introduction

In its dilute form, sulphuric acid reacts with metals (e.g. iron) through Equation (1) producing hydrogen (gas) and metal sulfate (salt) on the metal surface [1, 2, 3] given by Equation (1):

$$Fe_{(s)} + H_2SO_{4\ (aq)} = H_{2\ (g)} + FeSO_{4\ (aq)} \quad (1)$$

Recent advanced technology in crystallography and passivation film has identified key metallurgical parameters that can provide high corrosion resistance in acid solutions. Figure 1 shows an example of the in-laboratory behaviors of two cold-drawn low-carbon steel ASTM-179 tubes, with preferred versus unpreferred crystal grain orientation condition, after 15 h exposure to 6 % v/v **uninhibited** sulphuric acid at 60 °C and flow rate of 1 m/s. Significant corrosion of the unpreferred orientation (STD ASTM 179) with 94.3 wt% mass loss in comparison to the relatively unaffected preferred orientation (Superhex) with only 5.5 wt% mass loss.

Figure 1. Mass loss images of Superhex vs STD ASTM 179.

About 1000 tubes (lengths) of the Superhex material have been placed in each brand-new heat exchanger (HEX) unit and exposed to the alumina refinery process conditions as shown in Figure 2.

Figure 2. HEX unit tubed with Superhex.

2. Experimental

2.1 Sequency of Plant Operations

This is the list of process operations before acid cleaning.

- Drain Bayer liquor from the system.
- Water flush to remove residual liquor and line up valves and pumps to the acid circuit.
- Pump acid and recirculation.

2.2 Description of Electrochemistry Instrumentation

The corrosion setup used comprises a high-resolution potentiostat, multiplexer, data logger, laptop, and corrosion probe.

The potentiostat supplies the electronic signals for the corrosion cell. The multiplexer allows one to switch measurements from specimen to specimen and repeat them in a loop system. The data logger records the temperature across the whole process. The laptop drives the corrosion software and consequently controls all the instrumentation, and the corrosion probe holds the specimen under evaluation and exposes them to the real corrosion environment.

Figure 3. Instrument cabinet.

Figure 4. Corrosion probe.

Corrosion Probe: RP5

The sample holder has 5 positions (electrodes). P1, P2, and P4 positions for testing and the material are all low-carbon steel within the standard specification for seamless cold-drawn low-carbon steel heat exchangers and condenser tubes. The P3 and P5 positions for the reference and the counter electrode respectively to complete the electric circuit of the corrosion cell.
For this particular test, the positions description are as follows:

- P1 is occupied by a piece of tube corresponding to a material specified for alumina refineries.
- P2 is occupied by a piece of tube corresponding to the STD ASTM 179 (all purposes material).
- P4 is occupied by a piece of tube corresponding to the Superhex.

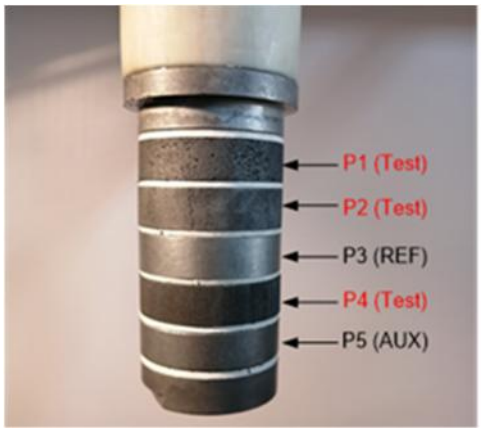

Figure 5. Sample holder.

2.3 Description of Electrochemistry Techniques

The above setup uses and measures corrosion using 3 corrosion techniques:

- The mass loss technique uses weight before and after exposure.
- LPR (Linear Polarization Resistance), uses direct current (DC) to measure the corrosion resistance of the material under evaluation.
- Impedance uses alternative current (AC) to measure the corrosion resistance of the material under evaluation. In this report, the author will use impedance data to highlight the corrosion resistance and LPR to calculate the corrosion rate (CR). In impedance, the corrosion resistance (Rp) is determined by the magnitude of the semicircle diameter of the Nyquist plot as shown in Figure 6.

The corrosion program has been set up to sequentially measure open circuit potential (OCP), LPR, and impedance in each specimen under evaluation and is done in approximately 6 minutes consequently, the measurements on the 3 specimens are completed in about 18 minutes and then repeated in a loop.

A run (loop) is defined as the consecutive measuring and completion of the 3 samples in the sample holder.

Note: As long as the specimens are in the same corrosion environment and measured consecutively, the magnitude of their corrosion resistances are comparative and inversely proportional to their corrosion rates at that specific time: higher corrosion resistance produces lower corrosion rate, consequently, less corrosion damage.

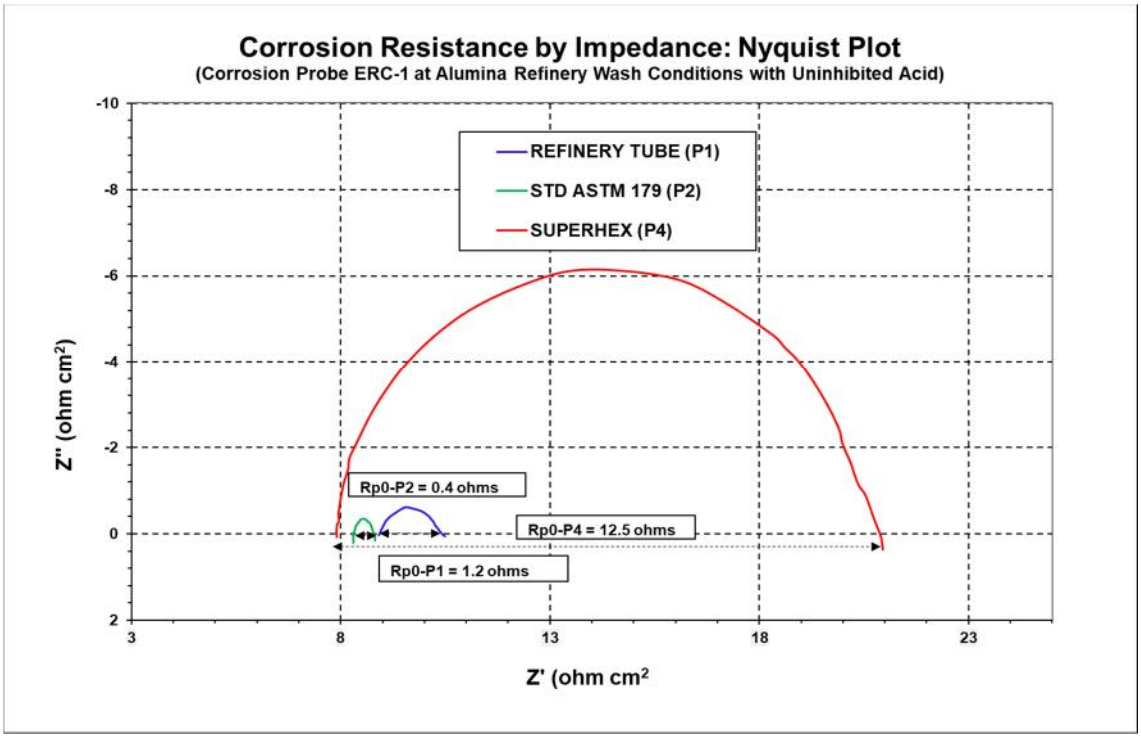

Figure 6. The Nyquist plot with uninhibited acid at washing conditions.

2.4 Calculation of Corrosion Rate

Polarization resistance (Rp), according to Faraday's law, is defined as the slope of potential vs current density given in Equation (2):

$$Rp = \frac{E}{i_{corr}} \tag{2}$$

where:
Rp Corrosion resistance
E Corrosion potential
i_{corr} Corrosion current

Corrosion current (i_{corr}) is then calculated according to the Stern-Geary relationship given in Equation (3):

$$i_{corr} = \left(\frac{\beta}{Rp}\right) \tag{3}$$

where:
β Stern-Geary coefficient determined as per Equation (4)
Rp Corrosion resistance obtained from LPR or impedance: (**Ω**)
i_{corr} Amp/cm^2

$$\beta = \frac{\beta a \cdot \beta c}{2.303 \cdot (\beta a + \beta c)} \tag{4}$$

where:
βa Anodic Tafel Slope

βc Cathodic Tafel Slope

Note

From Faraday's Law:

$$m = \frac{Ew \cdot Icorr \cdot t}{F} \quad (5)$$

where:
m Mass loss
Ew Fe equivalent weight = 28 g
t Time (year in s) = 31 536 000 s
F Faraday constant = 96 500

Mass Loss:

$$m = \rho \cdot V \quad (6)$$

Volume:

$$V = A \cdot d \quad (7)$$

where:
ρ Iron density = 7.86 g/cm^3
A Area exposed (input during measurement)
d CR = Corrosion thinning

So,

$$\rho \cdot A \cdot d = \frac{Ew \cdot Icorr \cdot t \times 10}{F} \quad (8)$$

$$\rho \cdot A \cdot d = \frac{Ew \cdot t \times 10}{F}\left(\frac{\beta}{R_p}\right) \quad (9)$$

$$d = \frac{Ew \cdot t \times 10}{F \cdot \rho}\left(\frac{\beta}{R_p \cdot A}\right) \quad (10)$$

$$Cfcorr = \frac{Ew \cdot t \times 10}{F \cdot \rho} \quad (11)$$

Note: When A (area) has been input in Cell Info to determine Rp, the area is not considered in (12).

$$CR = Cfcorr\left(\frac{\beta}{R_p}\right) \quad (12)$$

where:
Cfcorr Conversion factor determined as per Equation (11)
CR Millimetres/year (mmpy) (12)
Cfcorr 11 641.66

3. Results & Discussions

3.1 Overall Assessment of this Plant Trial During Acid Wash Using Impedance

The electrochemistry techniques used in this trial are genuine measurements of the instant corrosion behavior of the materials under the process line corrosion environment. Plant process conditions, such as suspended solids, and increased ionic impurities as a result of desilication product (DSP) dissolution, do not have any impact on the data collection quality.

However, flow dynamics through the pipe, such as air pockets in the liquid flow, intermittent flow velocity due to pump problems, etc, have a significant impact on the quality of data (noisy signal) especially when measuring impedance. This problem was observed in the low-frequency range of the measuring device (potentiostat) which corresponds to the high X-axis value of the Nyquist plot as shown in Figure 7.

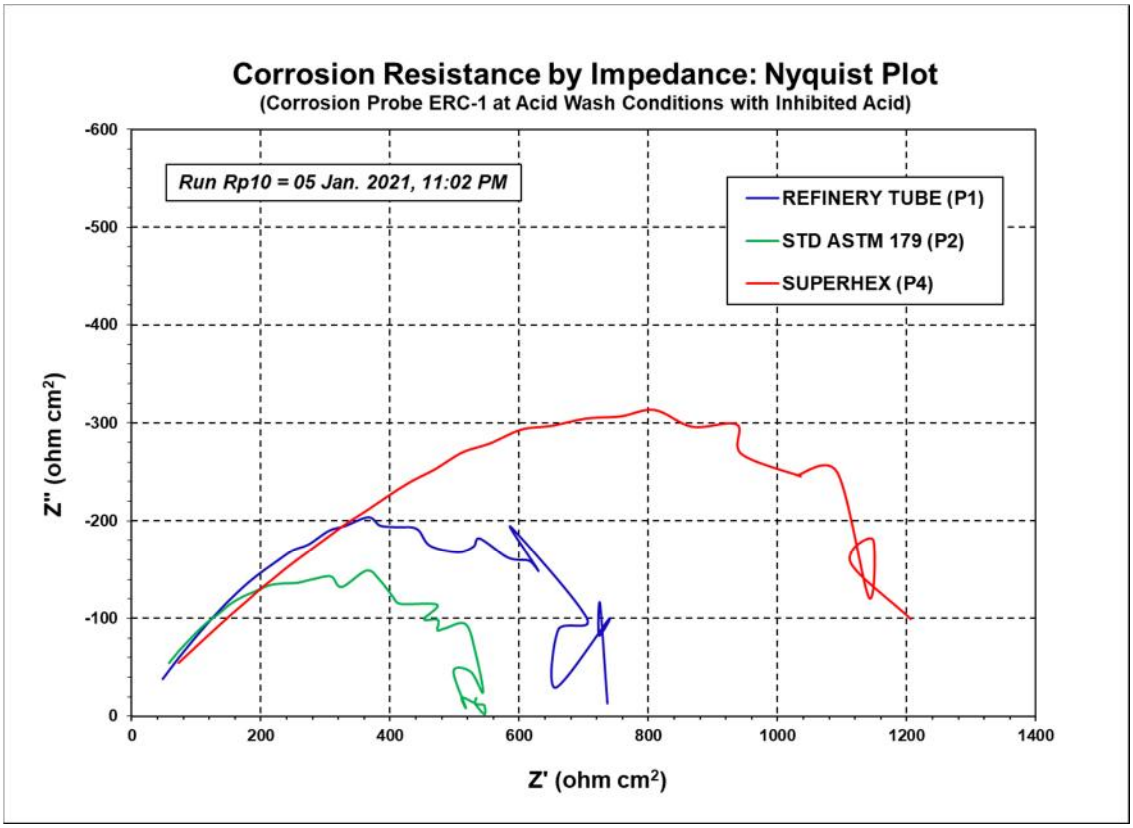

Figure 7. Plant data of Run Rp10.

The plot shown in Figure 8, is a laboratory replication (same plant temperature) of plant Run Rp10 using the same acid brew from Tk 30 before injection, and a replicated corrosion probe. This replication falls within the plant measurement range and removes the noise from the affected area during the plant run. Most of the runs carried out during this acid wash show the Superhex with higher corrosion resistance under real plant acid wash conditions as shown in Figures 7 & 8.

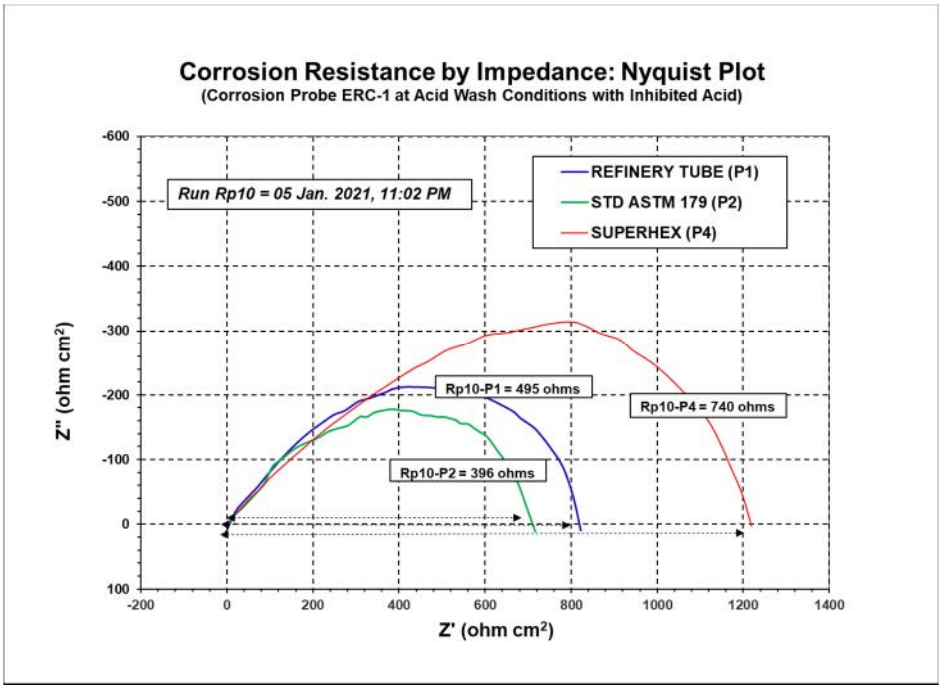

Figure 8. Laboratory data of Run Rp10 during acid washing.

3.2 Overall Assessment of this Plant Trial During Liquor Flow

The data collection during liquor flow showed less noise consequently, did not need correction. The data shows typical corrosion resistances during normal operations at full steam temperature conditions. The Nyquist plot semicircle is not completed due to the instrumentation set up however, the corrosion software can calculate corrosion resistance.

Most of the runs carried out during Bayer liquor show the Superhex with higher corrosion resistance as shown in Figure 9.

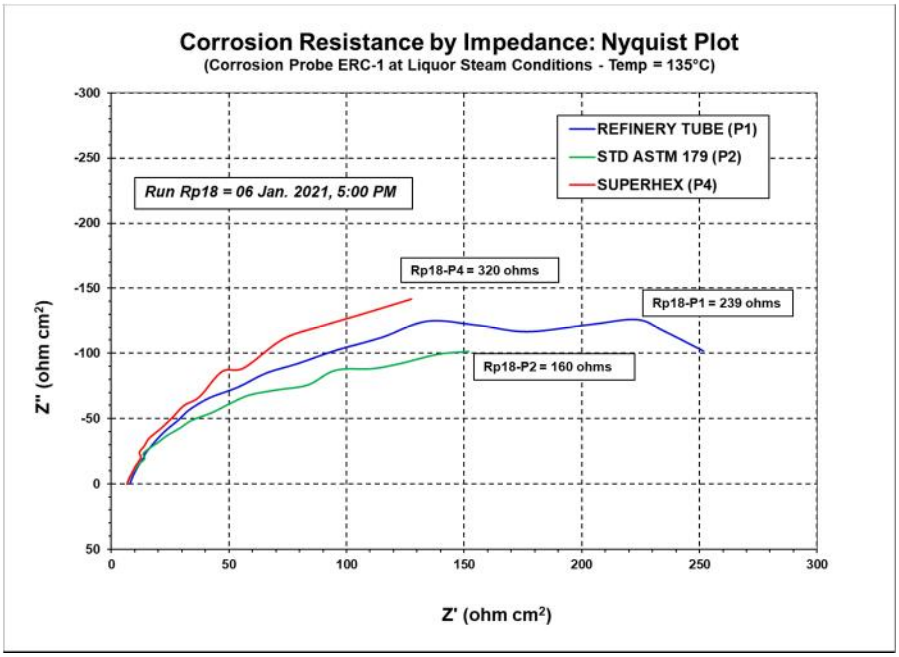

Figure 9. Plant data of Run Rp 18 during Bayer liquor flow.

3.3 Stern-Geary Coefficient

The Stern-Geary coefficient is required to express the data as corrosion rate and is experimentally determined (laboratory) by two techniques: Tefle's slope, shown in equation (4), and mass loss which uses LPR-generated data. Tafle's slopes are used for corrosion under Activation Mechanisms only and mass loss technique for any other corrosion mechanism that includes Diffusion Control of Cathodic Reaction.

This coefficient is specific for the corrosion environment in which the electrodes are and is dependent on the metal's metallurgical arrangement, such as orientation, type of electrolyte in contact with the metal surface, and temperature where the whole system is at.

The values in Table 1 were used in this report.

Table 1. Stern-Geary coefficients obtained from mass loss.

Stern-Geary Coeff.	Conditions	Refinery Tube QAL TO: 2205-01537	STD ASTM 179 Gove 13	Superhex PO: 0137
β	6% v/v Uninhibited H_2SO_4 Temp = 60 °C	**0.24012**	**0.58783**	**0.07570**
β	Plant Bayer Liquor at 135 °C	**0.01901**	**0.01572**	**0.00173**

Note: 1. Same values for inhibited acid at 60 °C
2. same values for plant Bayer liquor at 135 °C

3.4 Corrosion Rate During Acid Wash

LPR data was used to calculate the corrosion rate. Acid from TK 30 started being injected into the system on Tuesday 05/01/2021 at about 9:00 pm and finished at about 11:30 pm. This longer-than-usual injection time was due to operational problems not clearly explained to the author. Acid recirculation started immediately after this and finished on Wednesday 06/01/2021 at about 2:00 am.

The corrosion rates were kept between 0 and 5 mmpy along the injection and recirculation periods with pronounced spikes at the beginning of the injection period and less pronounced spikes afterward as shown in Figure 10.

Results depicted in Figure 10, indicate a satisfactory level of protection along the injection and recirculation stages. Corrosion rate values between 0 and 5 mmpy provide a well-inhibited system for low-carbon steel. A high corrosion rate at the beginning of the acid injection may indicate the depleted level of inhibition of the first acid reaching the probe as a result of the consumption on the whole metal surface before the probe. This is an inhibitor consumed on the piping surface between Tank 30 and the probe. This is, however, a short transition stage with a minor impact on the overall integrity of the HEX tube. Under these conditions, all materials under evaluation show a similar level of protection. The comparative behavior of Superhex against the other two tubes is distinctive. Superhex corroding at lower and more stable rates.

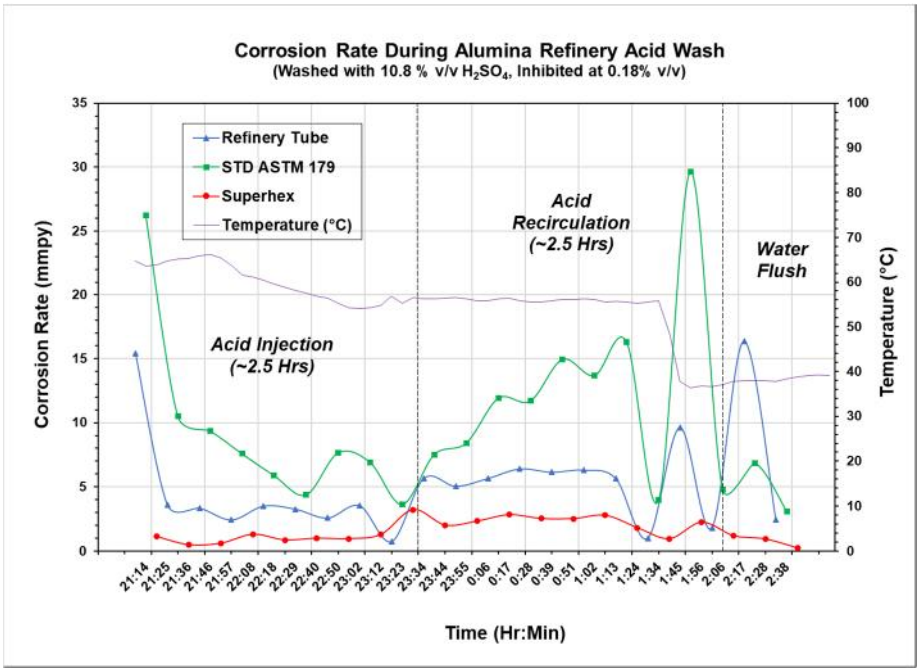

Figure 10. Corrosion rate during acid wash.

3.5 Corrosion Rate During Bayer Liquor Flow

After a few intents to start the liquor pump, it finally started injecting Bayer liquor into the system on Wednesday 06/01/2021 at about 1:22 pm starting at 75 °C. As the temperature increased, the corrosion rate tended to increase also reaching the highest value as steam was injected into the system. The corrosion rate levels were kept between 0 and 0.4 mmpy as shown in Figure 11. Results depicted in Figure 11, during liquor flow, indicate a satisfactory level of protection. Added to the inherent passive nature of caustic solution in low-carbon steel, the corrosion rates are kept between 0 and 0.4 mmpy.

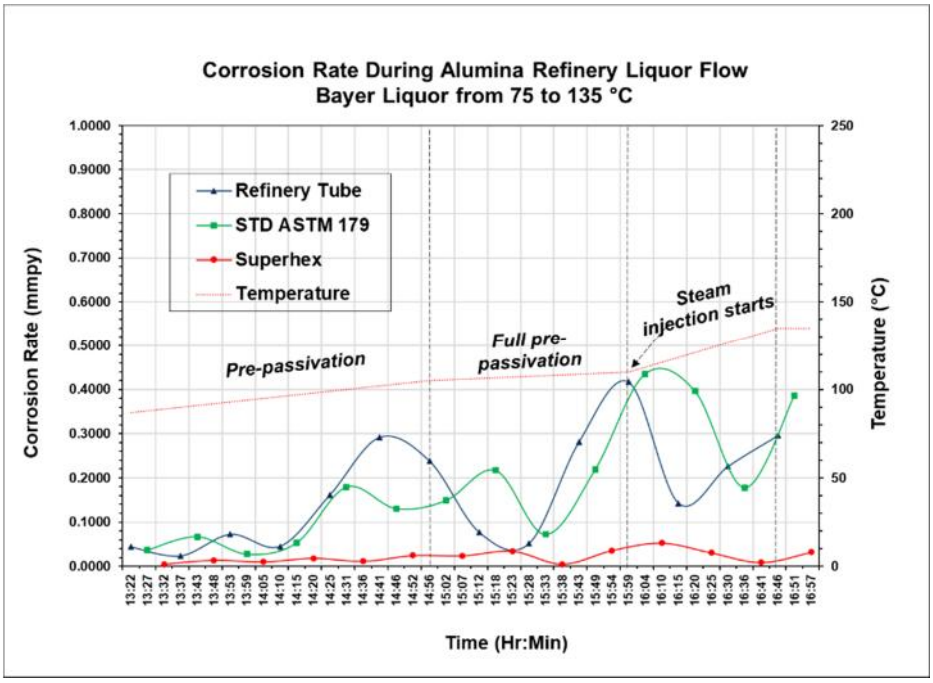

Figure 11. Corrosion rate during Bayer liquor flow.

Gradual increase of temperature during passivation and steam injection still brings the corrosion rate within acceptable levels. Under these conditions, the Superhex (red line) always shows the lowest corrosion rate and steadiest level of protection

3.6 Visual Inspection after One Year of Plant Exposure

After a year into operation, two HEX units tubed with Superhex and Alumina Refinery tubes respectively were opened for visual inspection. These two units were high-pressure life steam heaters (LSH) in a similar corrosion environment concerning temperature and pressure. During this time both units were exposed to the same process conditions and had the same acid washes as part of the acid cleaning schedule.

The Alumina Refinery Tube (Figure 12) showed a heavy corrosion attack at the end of the tubes protruding from the tube sheet, not able to see along the length of the tube (middle section). On the other hand, the Superhex (Figure 13) appears to be intact.

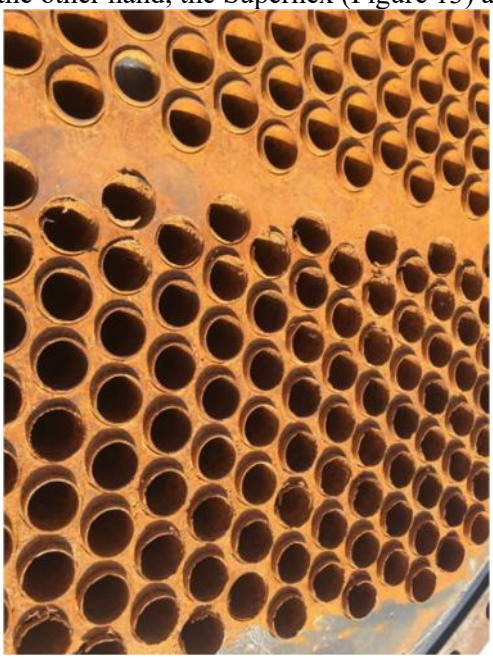

Figure 12. Alumina refinery tube.

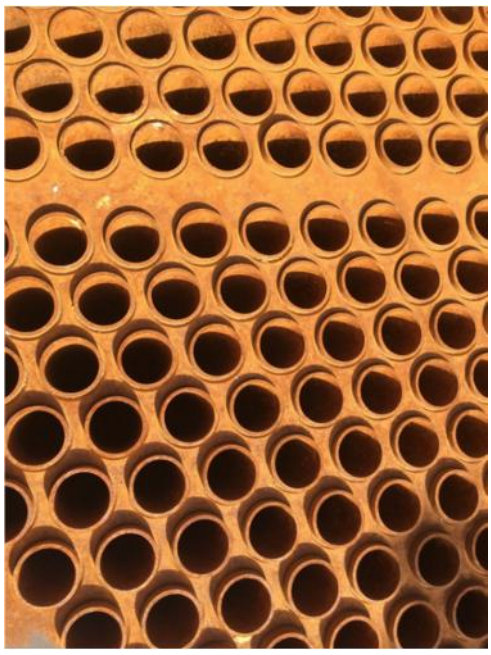

Figure 13. Superhex tube.

3.7 Dose Response of Corrosion Inhibitor PIC 515

This is laboratory-generated data that depicts the degree of adsorption on the metal material as the dose of corrosion inhibitor is increased from no protection to a fully protected condition. This test was performed at refinery acid-cleaning conditions.

As seen in Figure 14, the three materials under evaluation have different levels of adsorption at the beginning of the trends and they tend to equal and reach full inhibition levels as the dose increases. It can also be observed that metal materials reach maximum protection (lower corrosion rate) at a certain dosage and beyond that, additional corrosion inhibitor does not provide any extra protection.

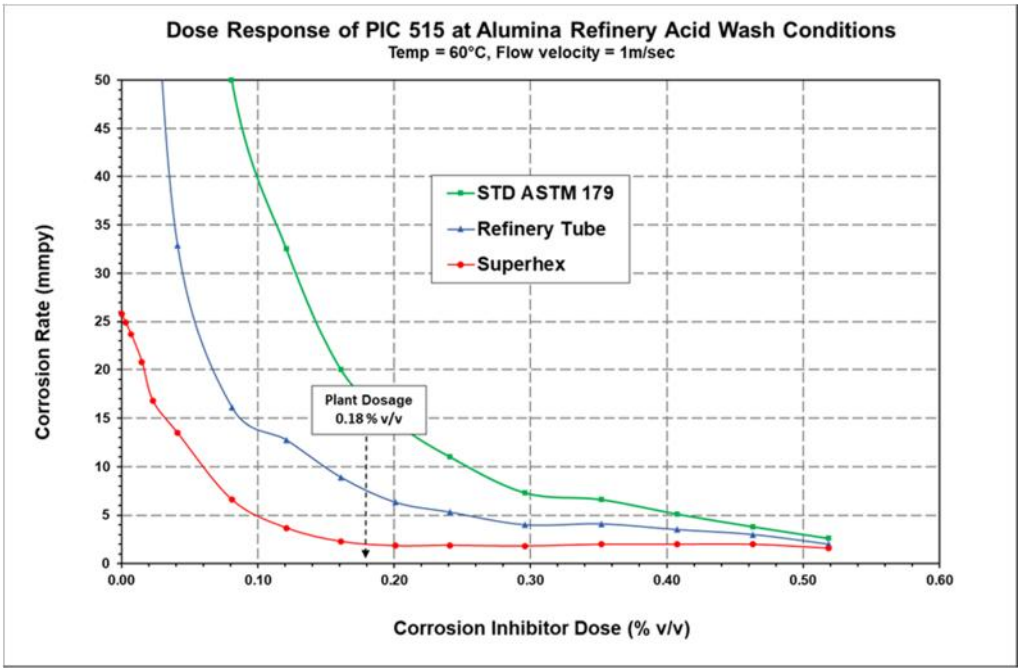

Figure 14. Laboratory dose response of corrosion inhibitor PIC 515.

PIC 515 has been formulated as a dispersible but not fully soluble substance in aqueous solutions. Liquids of this nature, once reaching high concentrations, tend to come up to the top and concentrate at the water surface when there is not enough agitation.

The experimental work depicted in Figure 14 has reached a maximum dose of 0.5188 % v/v and did not show corrosion inhibitors concentrated on the water surface. This may indicate that the acid brew used on 05/01/2021 more likely was overdosed above 0.5188 % v/v.

3.8 Temperature Response of Corrosion Inhibitor PIC 515

This is also laboratory-generated data that shows how strong the corrosion inhibitor adsorption onto the metal surface is as the temperature increases. The test was done at a complete inhibition level, in this case, 0.18 % v/v, and then the temperature was gradually increased to a level where the corrosion rates compromised the integrity of the HEX tube (see Figure 15).

As per trends depicted in Figure 13, temperature has a great effect on the corrosion rate and this is related to the chemical formulation of the corrosion inhibitor and the metallurgy of the metal surface.

In most of the corrosion systems of diluted acids, the corrosion rate becomes exponential as the temperature increases. Most of the more effective corrosion inhibitors used in acid solutions are organic base chemicals. Some organic chemicals break down the carbon chain under temperature and lose their property as effective corrosion inhibitors. The metallurgy of the metal surface about microstructure and chemical composition is strongly related to the degree of adsorption.

As we see in Figure 14, Superhex performs better with the current corrosion inhibitor by providing strong adsorption up to 70 °C.

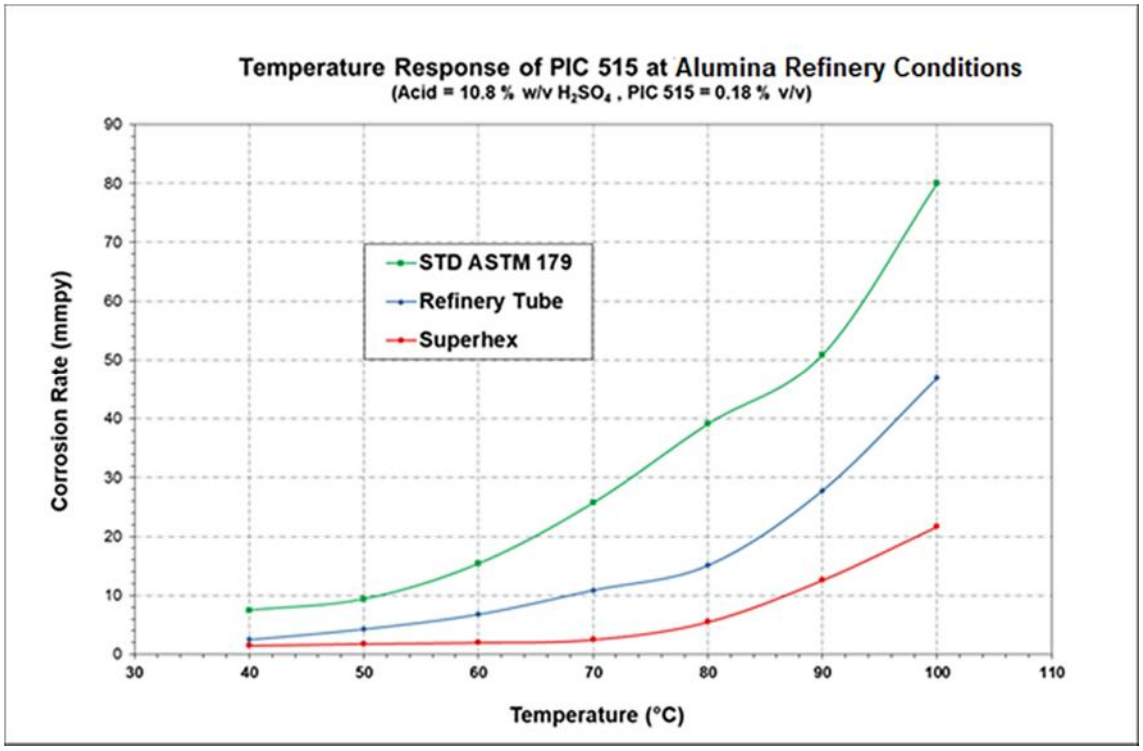

Figure 15. Laboratory temperature response of corrosion inhibitor PIC 515.

4. General Comments and Room for Improvement

Superhex will provide a solid backup to the current operational acid washing procedure due to its high corrosion resistance to uninhibited and inhibited diluted sulphuric acid and good surface adsorption to the current corrosion inhibitor PIC 515.

Corrosion inhibitors are key components to minimize corrosion damage to low-carbon steel exposed to diluted sulphuric or hydrochloric acid. All alumina refineries use corrosion inhibitors to protect their HEX tube exposed during acid wash. The reality is, under this protected environment, the range of life span of their HEX tubes varies from 3 to 5 years (digestion heaters) which is considered low. The tube life span of the tube should be above 5 years. This indicates that the high level of protection given by the inhibitor at a particular time is not kept during the operational life of the tube. Appears to be that the inhibitor protection has not always been there as it should be, as a result, various degrees of corrosion damage has always happened. A high corrosion resistance material based on its inner metallurgy, such as the Superhex, will always be there to mitigate corrosion attack and will enhance the protection with a suitable corrosion inhibitor and reach life spans well beyond 5 years.

The data obtained on this plant trial and the related laboratory tests highlight the fact that there is room for improvement within the current procedure of acid washing.

5. References

1. M.G. Fontana, *Corrosion engineering*, 3rd Edition, McGraw-Hill Book Company, 1985.
2. M.J. King, W.G. Davenport, M.S. Moats, Materials of construction, sulfuric acid manufacture - analysis, control, and optimization,2nd Edition, *Elsevier*, San Diego, Calif, 2013, pp. 349-356.
3. S. Lyon, Overview of corrosion engineering, science and technology, *Nuclear Corrosion Science and Engineering*, Elsevier Ltd2012, pp. 3-30.

4. F. Mansfeld, Tafel slopes and corrosion rates obtained in the pre-Tafel region of polarization curves, *Corrosion Science*, 47 (2005) 3178-3186.
5. ASTM G102-89(2015)e1, Standard practice for calculation of corrosion rates and related information from electrochemical measurements, *ASTM International*, West Conshohocken, PA, 2015.
6. ASTM G59-97(2014), Standard test method for conducting potentiodynamic polarization resistance measurements, *ASTM International*, West Conshohocken, PA, 2014.
7. ASTM G3-14, Standard practice for conventions applicable to electrochemical measurements in corrosion testing, *ASTM International*, West Conshohocken, PA, 2014.
8. K. Vignarooban et al., Corrosion resistance of Hastelloy in molten metal-chloride heat-transfer fluids for concentrating solar power applications, *Solar Energy*, 103 (2014) 62-69.
9. *The modified inductance element La*, Application Note 42, Bio-Logic Science Instruments, 2012.
10. S. Ramanathan, Negative resistances and inductances in equivalent circuits for adsorption-reaction kinetics, *ECS Transactions*, 33 (2011) 21-35.
11. C. Gabrielli, M. Keddam, H. Takenouti, *The use of a.c. techniques in the study of corrosion and passivity*, 23 (1983) 395-451.
12. D. Clover et al., The influence of microstructure on the corrosion rate of various carbon steels, *J Appl Electrochem*, 35 (2005) 139-149.
13. Q.Y. Pan et al., The improvement of localized corrosion resistance in sensitized stainless steel by laser surface remelting, *Surface and Coatings Technology*, 102 (1998) 245-255.
14. J.P. Diard et al., Calculation, simulation, and interpretation of electrochemical impedance. Part II. Interpretation of Volmer-Heyrovsky impedance diagrams, *Journal of Electroanalytical Chemistry and Interfacial Electrochemistry*, 255 (1988) 1-20.
15. F. Mansfeld, Analysis, and interpretation of EIS data for metals and alloys, *Technical Report No. 26, University of Southern California*, Los Angeles, CA, USA, 1999.
16. H.P. Stüwe, A.F. Padilha, F. Siciliano, Competition between recovery and recrystallization, *Materials Science and Engineering: A*, 333 (2002) 361-367.
17. D. Raabe, Recovery and recrystallization: phenomena, physics, models, simulation, in D.E.L. Hono (Ed.) *Physical Metallurgy (Fifth Edition)*, Elsevier, Oxford, 2014, pp. 2291-2397